# $^{171}$Yb Cross-Polarization Magic Angle Spinning NMR Spectroscopic Studies of Organometallic Compounds: Bis(cyclopentadienyl) Derivatives

Julian M. Keates and Gerard A. Lawless*

*The Chemistry Laboratory, School of Chemistry, Physics and Environmental Science, University of Sussex, Brighton BN1 9QJ, U.K.*

*Received January 14, 1997*[⊗]

A series of nine Yb(II) bis(cyclopentadienyl) complexes have been studied by $^{171}$Yb CP MAS (cross polarization magic angle spinning) NMR spectroscopy. The optimization of the cross polarization conditions are described. The proton $T_{1\rho}$ values have been determined. The spinning side band manifold for each compound has been analyzed. The derived chemical shift tensor data are discussed with respect to molecular structure elucidation.



## Introduction

The chemistry of the +II oxidation state derivatives of the lanthanides Sm, Eu, and Yb is of continuing interest due to their unique reactivity.[1] A wide range of $YbL_2$-type complexes, including, for example, alkoxides and siloxides,[2] aryloxides,[3,4] alkyls,[5] amides,[6] cyclopentadienyls,[7,8] phospholes,[9] silyls,[10] stannyls,[11] and thiolates,[12] have been reported. Of these complexes, the bis(cyclopentadienyl) derivatives have been the most widely studied with respect to catalysis and small molecule activation, while the alkoxides have attracted much attention as precursors to high $T_c$ superconductor materials. Exploration of the Yb(II) oxidation state has been considerably facilitated by the development of high-resolution solution-state $^{171}$Yb NMR spectroscopy.[13] The number of $^{171}$Yb chemical shifts reported to date exceeds 200, with a corresponding chemical shift dispersion of some 3000 ppm (from *ca.* $\delta$ +2500 to −500 ppm). Coupling constant data have been reported for $^{171}$Yb to $^{1}$H,[14−16] $^{13}$C,[17,18] $^{14}$N,[13] $^{29}$Si,[10] $^{31}$P,[9,16] $^{117/119}$Sn,[11] and $^{125}$Te.[19] In many of these solution-state studies, large temperature dependencies for both the chemical shift, $\delta$, and linewidths at peak half-heights, $\nu_{1/2}$, have been observed, often resulting from complicated equilibria between, for example, complexes with varying degrees of solvation, monomer−dimer equilibria, reversible salt addition reactions, or reactions with the solvent itself. In some cases, $^{171}$Yb shifts also depend on concentration and, of course, the solvent employed. Though for many organometallic ytterbium(II) compounds molecular solid-state structures have been determined, the extrapolation of such data for these compounds to the solution state is often tenuous. Solid-state $^{171}$Yb NMR spectroscopic data provides a means of both elucidating the structural relationship between the solution and solid state and facilitating the characterization of the many noncrystalline ytterbium(II) compounds. To date three wide-line solid-state studies of the $^{171}$Yb nucleus have been reported.[20−22] More recently, the static and magic angle spinning spectra, MAS, of $RbYbI_3$ have been described.[23] We now report the study of a series of Yb(II) bis(cyclopentadienyl) derivatives by solid-state $^{171}$Yb NMR spectroscopy. A preliminary communication of this work[24] and another shorter account[25] have recently been reported.

## Experimental Section

All compounds were handled with the rigorous exclusion of air and water using standard Schlenk techniques. All solvents were freshly distilled and dried by reflux over sodium or sodium−potassium alloy under a dinitrogen atmosphere.

[⊗] Abstract published in *Advance ACS Abstracts,* May 15, 1997.

(1) Evans, W. J.; Grate, J. W.; Doedens, R. J. *J. Am. Chem. Soc.* **1985**, *107*, 1671−1679.
(2) Duncalf, D. J.; Hitchcock, P. B.; Lawless, G. A. *J. Chem. Soc., Chem. Commun.* **1996**, 269−271.
(3) van den Hende, J. R.; Hitchcock, P. B.; Lappert, M. F. *J. Chem. Soc., Chem. Commun.* **1994**, 1413−1414.
(4) van den Hende, J. R.; Hitchcock, P. B.; Holmes, S. A.; Lappert, M. F. *J. Chem. Soc., Dalton Trans.* **1995**, 1435−1440.
(5) Hitchcock, P. B.; Holmes, S. A.; Lappert, M. F.; Tian, S. *J. Chem. Soc., Chem. Commun.* **1994**, 2691−2692.
(6) Tilley, T. D.; Andersen, R. A.; Zalkin, A. *Inorg. Chem.* **1984**, *23*, 2271−2276.
(7) Andersen, R. A.; Boncella, J. M.; Burns, C. J.; Green, J. C.; Hohl, D.; Rösch, N. *J. Chem. Soc., Chem. Commun.* **1986**, 405−407.
(8) Schwartz, D. J.; Anderson, R. A. *Organometallics* **1995**, *14*, 4308−4318.
(9) Nief, F.; Ricard, L.; Mathey, F. *Polyhedron* **1993**, *12*, 19−26.
(10) Corradi, M. M.; Frankland, A. D.; Hitchcock, P. B.; Lappert, M. F.; Lawless, G. A. *J. Chem. Soc., Chem. Commun.* **1996**, 2323−2324.
(11) Cloke, F. G. N.; Dalby, C. I.; Hitchcock, P. B.; Karamallakis, H.; Lawless, G. A. *J. Chem. Soc., Chem. Commun.* **1991**, 779−781.
(12) Çetinkaya, B.; Hitchcock, P. B.; Lappert, M. F.; Smith, R. G. *J. Chem. Soc., Chem. Commun.* **1992**, 932−934.
(13) Avent, A. G.; Edelmann, M. A.; Lappert, M. F.; Lawless, G. A. *J. Am. Chem. Soc.* **1989**, *111*, 3423−3425.
(14) Takats, J.; Zhang, X. W.; Bond, A. H.; Rogers, R. D. *New J. Chem.* **1995**, *19*, 573.
(15) Hasinoff, L.; Takats, J.; Zhang, X. W.; Bond, A. H.; Rogers, R. D. *J. Am. Chem. Soc.* **1994**, *116*, 8833−8834.
(16) Green, M. L. H.; Hughes, A. K.; Michaelidou, D. M.; Mountford, P. *J. Chem. Soc., Chem. Commun.* **1993**, 591−593.
(17) Dalby, C. I. Ph.D. Thesis, University of Sussex, Brighton, U.K., 1993.
(18) Eaborn, C.; Hitchcock, P. B.; Izod, K.; Smith, J. D. *J. Am. Chem. Soc.* **1994**, *116*, 12071−12072.
(19) Strzelecki, A. R.; Likar, C. L.; Helsel, B. A.; Utz, T.; Lin, M. C.; Bianconi, P. A. *Inorg. Chem.* **1994**, *33*, 5188−5194.
(20) Gossard, A. C.; Jaccarion, V.; Wernick, J. H. *Phys. Rev.* **1964**, *133*, 881.
(21) Zogal, O. J.; Stalinksi, B. *Magn. Reson. Relat. Phenom., Proc. Cong. Ampere, 20th*, **1978**, 433.
(22) Shimiza, T.; Takigowa, M.; Yasuoka, H.; Wernick, J. H. *J. Magn. Magn. Mater.* **1985**, *52*, 187.
(23) Mao, X.-A.; Zhao, X.; Ye, C.; Wang, S. *Solid State Nucl. Magn. Reson.* **1994**, *3*, 107−110.
(24) Keates, J. M.; Lawless, G. A.; Waugh, M. P. *J. Chem. Soc., Chem. Commun.* **1996**, 1627−1628.
(25) Rabe, G. W.; Sebald, A. *Solid State Nucl. Magn. Reson.* **1996**, *6*, 197−200.

S0276-7333(97)00022-8 CCC: $14.00 

[Yb($\eta$-$C_5Me_5$)$_2$($OEt_2$)] **(6)** was prepared according to a literature method[26] and was the precursor for the other solvates [Yb($\eta$-$C_5Me_5$)$_2$($THF$)$_2$] **(2)**, [Yb($\eta$-$C_5Me_5$)$_2$($py$)$_2$] **(3)**,[27] and [Yb($\eta$-$C_5Me_5$)$_2$(DME)] **(4)**.[28] The base-free compound [Yb($\eta$-$C_5Me_5$)$_2$] **(9)**[29] was prepared *via* repeated sublimations of the ether solvate. [Yb($\eta$-$C_5Me_4H$)$_2$($THF$)$_2$] **(1)** was prepared from $YbI_2$ and Na($C_5Me_4H$) in THF.[30] Yb($\eta$-$Cp^s$)$_2$ [$Cp^s$ = $C_5Me_4$($SiMe_2$-$Bu^t$)] **(8)** was prepared from $YbI_2$ and 2 equiv of $NaCp^S$ in toluene.[31] [Yb($\eta$-$C_5Me_4SiMe_3$)$_2$($THF$)] **(5)** was prepared from $YbI_2$($THF$)$_2$ and 2 equiv of Na($C_5Me_4SiMe_3$) in $Et_2O$.[32] All samples were additionally characterized by $^1$H and $^{13}$C NMR spectroscopies and mass spectroscopy. CP, CP MAS, and MAS $^{171}$Yb NMR spectra were obtained on a Bruker DMX-400 spectrometer equipped with a 9.4 T magnet and a 4 mm variable-temperature double-bearing probe. Samples (100−150 mg) were ground in a glovebox operating at <1 ppm $H_2O$ and <1 ppm $O_2$ and packed into Zirconia rotors with a Kel-F end cap. Samples were spun at the magic angle, set using KBr,[33] with $N_2$. No sample decomposition was observed. Spin rates, $\nu_r$, between 2.5 and 15 kHz were utilized. Sample temperatures were 298 ± 2 K. A single-contact cross polarization, CP, pulse sequence was used to acquire all static and MAS $^{13}$C and $^{171}$Yb spectra. At elevated spin rates (≥6 kHz) a ramped-amplitude contact pulse was used (triangular ramp ±25%, 128 data points).[34] High-power $^1$H decoupling was used in all experiments. The $^{171}$Yb−$^1$H cross-polarization contact time, 9 ms, was optimized for **2** with $\nu_r$ = 7.5 kHz *(vide infra)*. For $^{13}$C−$^1$H cross-polarization experiments, a contact time of 3 ms was employed. The 90° proton pulse width was calibrated to 3.9 $\mu$s. Prescan delays of between 5 and 7 s were used. Spectral widths were typically 80−140 kHz. Between 1024 and 4096 complex data points were acquired. Backwards linear prediction, BLP, was used, where necessary. Ytterbium chemial shifts were referenced to the absolute resonance frequency of $^{171}$Yb in a THF solution of **2**. Carbon chemical shifts were referenced to the high-frequency $CH_2$ peak of adamantane, $\delta$ = 38.4.

## Results and Discussion

**Hartmann−Hahn Matching.** The advantages of cross polarization are well-documented.[35] For ytterbium, the theoretical sensitivity enhancement is 5.7. In addition to being the reference compound for solution-state $^{171}$Yb NMR spectroscopy, we chose **2** to set the Hartmann−Hahn condition since (i) its line width at peak half-height, $\nu_{1/2}$, is small (170 Hz), (ii) it exhibits good cross-polarization dynamics *(vide infra)*, and (iii) the unremarkable proton relaxation rates permit relatively short delays between scans. These properties fufill the criteria for an "ideal" standard compound to set up the Hartmann−Hahn matching condition for CP.[36] Spectra were acquired using a 90° proton pulse of 3.9 $\mu$s and a 6 s relaxation delay. A standard single-contact CP pulse sequence with high-power proton decoupling was employed. With the contact time set to 10 ms, the $^{171}$Yb channel power was gradually increased until a maximum signal intensity was obtained. Adequate signal-to-noise ratios were achieved with 32 transients acquired. The Hartmann−Hahn condition was initially set for a sample with a rotation rate of 7.0 kHz and showed no significant variation when adjusted for three other samples ([Yb($\eta$-$C_5Me_4H$)$_2$($THF$)$_2$], [Yb($\eta$-$C_5Me_5$)$_2$(DME)], and [Yb($\eta$-$C_5Me_5$)$_2$($Et_2O$)]). An alternative approach for setting the Hartmann−Hahn match at lower magnetic field strengths has been reported.[25] At a field of 2.35 T, the Larmor frequencies of $^{171}$Yb and $^{199}$Hg differ by less than 0.5 MHz (17.5 and 17.9 MHz, respectively) and the Hartmann−Hahn match was found using Hg($O_3SCF_3$)$_2$($DMSO$)$_6$.

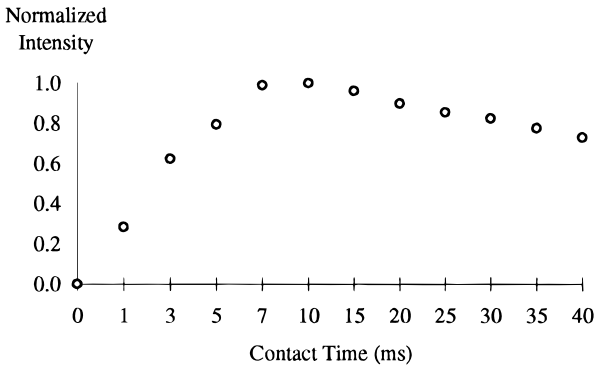


**Figure 1.** Contact time optimization for **2** at $\nu_r$ = 7 kHz.

**Contact Time Optimization.** For a sample of **2** spinning at 7 kHz, spectra were acquired with contact times which varied from 1 $\mu$s to 40 ms.[37] A maximum signal-to-noise ratio was observed when a contact time of *ca*. 9 ms was employed (Figure 1). This value is comparable with those found in other organometallic systems ($^{89}$Y 1−20 ms;[38] $^{119}$Sn 5 ms,[39] 5−20 ms;[40] $^{207}$Pb 5 ms,[41] 10 ms;[40] $^{113}$Cd 3.45 ms,[42] 10 ms[43]). Since the decay of intensity after the maximum is due to a decay of the proton spin magnetization arising from relaxation in the rotating frame, a lower limit for the most efficient $T_{1\rho}$ relaxation mechanism must be *ca*. 10 ms.

***$T_{YbH}$* and *$T_{1\rho}$*.** The ytterbium−proton cross-relaxation (cross-polarization) time, $T_{YbH}$, and the proton spin−lattice relaxation time in the rotating frame are intimately related to the cross-polarization process. $T_{YbH}$ determines the rate at which polarization can be transferred from the abundant $^1$H spins to the rarer $^{171}$Yb spins. In contrast, the rotating frame spin−lattice relaxation rate, $T_{1\rho}$, determines not only the maximum contact time, but also whether multiple contacts are feasible. For **2**, all three proton environments, each characterized by an individual $T_{1\rho}$ value, will contribute to the overall $T_{1\rho}$. In principle, this overall $T_{1\rho}$ could be determined *via* $^{171}$Yb NMR spectroscopy but since in the $^{13}$C CP MAS spectrum all three C−H resonances

(26) Tilley, T. D.; Boncella, J. M.; Berg, D. J.; Burns, C. J.; Andersen, R. A. *Inorg. Synth*. **1990**, *27*, 146−150.
(27) Tilley, T. D.; Andersen, R. A.; Spencer, B.; Zalkin, A. *Inorg. Chem*. **1982**, *21*, 2647−2649.
(28) Duncalf, D. J. Ph.D. Thesis, University of Sussex, Brighton, U.K., 1994.
(29) Burns, C. J. Ph.D. Thesis, University of California, Berkeley, CA, 1987.
(30) Schumann, H.; Glanz, M.; Hemling, H.; Hahn, F. E. *Z. Anorg. Allg. Chem*. **1995**, *621*, 341−345.
(31) Constantine, S. P.; Lawless, G. A. Unpublished results.
(32) Keates, J. M.; Lawless, G. A. Unpublished results.
(33) Frye, J. S.; Maciel, G. E. *J. Magn. Reson. A* **1982**, *48*, 125−131.
(34) Metz, G.; Wu, X.; Smith, S. O. *J. Magn. Reson. A* **1994**, *110*, 219−227.
(35) Stejskal, E. O.; Schaefer, J.; Waugh, J. S. *J. Magn. Reson. A* **1977**, *28*, 105.
(36) Harris, R. K.; Sebald, A. *Magn. Reson. Chem*. **1987**, *25*, 1058−1062.
(37) Other significant parameters include a 6 s recycle delay and 32 transients acquired.
(38) Wu, J.; Boyle, T. J.; Shreeve, J. L.; Ziller, J. W.; Evans, W. J. *Inorg. Chem*. **1993**, *32*, 1130−1134.
(39) Reger, D. L.; Huff, M. F.; Knox, S. J.; Adams, R. J.; Apperley, D. C.; Harris, R. K. *Inorg. Chem*. **1993**, *32*, 4472−4473.
(40) Harris, R.; Sebald, A. *Magn. Reson. Chem*. **1989**, *27*, 81−87.
(41) Janiak, C.; Schumann, H.; Stader, C.; Wrackmeyer, B.; Zuckerman, J. J. *Chem. Ber*. **1988**, *121*, 1745−1751.
(42) Kennedy, M. A.; Ellis, P. D.; Jakobsen, H. J. *Inorg. Chem*. **1990**, *29*, 550−552.
(43) Sardashti, M.; Maciel, G. E. *J. Magn. Reson. A* **1987**, *72*, 467−474.

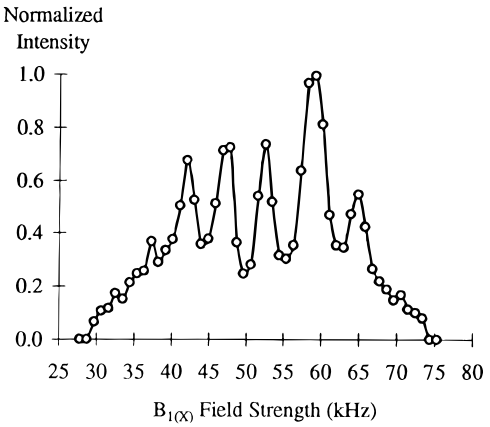


**Figure 2.** The $^{171}$Yb Hartmann−Hahn spectrum of **2** at $\nu_r = 7$ kHz.

**Table 1. Proton Rotating Frame Spin−Lattice Relaxation Data, $T_{1\rho}$, for 2**

| $^{13}$C chemical shift ($\delta$) | $T_{1\rho}$ (ms) | proton environment |
|---|---|---|
| 72 | 10.9 | $\alpha$-$CH_2$ (THF) |
| 27 | 23.8 | $\beta$-$CH_2$ (THF) |
| 13 | 40.1 | $CH_3$ |

are unique, it was possible to determine their individual $T_{1\rho}$ values[44] (Table 1). The shortest $T_{1\rho}$ of 10.9 ms agrees well with that predicted from Figure 1. All three values are within the range typical for $^1$H $T_{1\rho}$ (5−50 ms).[45]

**CP and RAMP-CP.** Two difficulties associated with nuclei which exhibit large chemical shift anisotropy, CSA, are (i) the potential for deviations in the intensity distribution of spinning side band manifolds, SSB,[46] and (ii) the increased sensitivity of the Hartmann−Hahn match at the relatively high rotation rates commonly employed during the observation of such nuclei. Under MAS, optimal CP transfer occurs when $\omega_{1Yb} = \omega_{1H} \pm n\nu_r$.[35,47,48] A series of $^{171}$Yb CP MAS spectra of **2** were acquired with increasing $\omega_{1Yb}$ and with $\nu_r = 7.0$ kHz.[49] The resulting intensities of the isotropic resonance are shown in Figure 2 and display the expected maxima resulting from the modulation of the dipolar interaction by MAS. Furthermore, by inspection, the magnitude of the $^{171}$Yb−$^1$H dipolar interaction can be estimated as *ca*. 26 kHz. The origin of the intensity distortion for $\omega_{1Yb} = \omega_{1H} + \nu_r$ and $\omega_{1Yb} = \omega_{1H} + 2\nu_r$ is unclear but may arise from RF inhomogeneity.[50] The dependence of the CP condition on $\nu_r$ may be minimized by employing a ramped-amplitude cross-polarization sequence, RAMP-CP.[34] CP and RAMP-CP spectra were acquired for several compounds using different rotation rates, $\nu_r$. Typically, as shown for **2** (Figure 3), when $\nu_r > 6$ kHz,

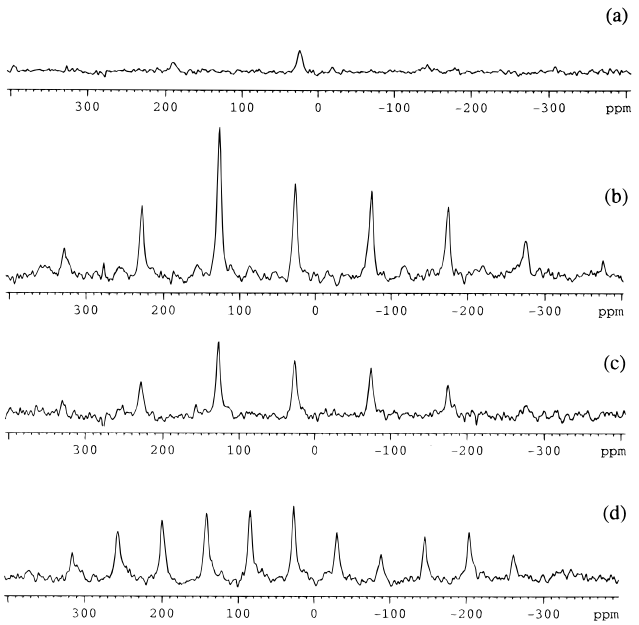


**Figure 3.** $^{171}$Yb spectra of **2** (a) MAS 11.5 kHz, 256 transients, 30 s interscan delay, S:N = 7; (b) RAMP-CP 7 kHz, 1024 transients, 6 s interscan delay, S:N = 21; (c) CP 7 kHz, 1024 transients, 6 s interscan delay, S:N = 10; (d) CP 4 kHz, 1024 transients, 6 s interscan delay, S:N = 13. All acquisition periods equaled 100 min. Spectra are shown with comparable intensity axes. S:N was calculated according to S:N = {(maximum signal intensity)/2 × variance of noise intensity}.

the S:N ratio of the CP spectra decreased, whereas for the RAMP-CP spectra, the S:N ratios remained constant up to spin rates of 11 kHz.

**Spinning Sideband Manifold Analyses.** Spinning sideband manifolds were analyzed by the methods of both Herzfeld and Berger and of Maricq and Waugh.[51,52] Both methods are subject to error, particularly when the symmetry of the tensor approaches axial[53] or when too few sidebands are analyzed.[54] In view of these problems, static CP spectra were also acquired for **1** and **2**. Figure 4 shows the spectra for the former, but both gave excellent agreement for the principal components of the chemical shift, as determined by computer fitting (Table 2). The principal components of the chemical shift tensor for **1**−**9**, together with derived values for anisotropy, $\Delta_\sigma$, asymmetry, $\eta$, span, $\Omega$, and skew, $\kappa$, are listed in Table 3.[55] Values are shown as chemical shifts, but chemical shielding values ($\delta = -\sigma$; $\sigma_{11} < \sigma_{22} < \sigma_{33}$; $\delta_{11} > \delta_{22} > \delta_{33}$)[56] have been used to calculate the anisotropy and asymmetry parameters where appropriate. A selected series of typical CPMAS spectra for **4**, **5**, and **8** are presented in Figure 5.

(44) $^{13}$C CP MAS spectra were acquired for a sample of [Yb($\eta$-$C_5Me_5$)$_2$(THF)$_2$] with $\nu_r = 7.0$ kHz. Thirty two transients were acquired for each increment (1 $\mu$s, 1, 2, 5, 10, 20, 30, 40 ms). The data were fitted to a single exponential decay using the simfit routine of the XWINNMR package.

(45) Schumann, H.; Meese-Marktscheffel, J. A.; Dietrich, A.; Pickardt, J. *J. Organomet. Chem.* **1992**, *433*, 241−252.

(46) Jeschke, G.; Grossmann, G. *J. Magn. Reson. A* **1993**, *103*, 323−328.

(47) Wind, R. A.; Dec, S. F.; Lock, H.; Maciel, G. E. *J. Magn. Reson. A* **1988**, *79*, 136−139.

(48) Jakobsen, H. J.; Daugaard, P.; Langer, V. *J. Magn. Reson. A* **1988**, *76*, 162−168.

(49) Other significant parameters include a 9 ms contact time, a 6 s recycle delay, and 256 transients acquired.

(50) Kolbert, A. C.; Bielecki, A. *J. Magn. Reson. A* **1995**, *116*, 29−35.

(51) Herzfeld, J.; Berger, A. E. *J. Chem. Phys.* **1980**, *73*, 6021−6030.

(52) Maricq, M. M.; Waugh, J. S. *J. Chem. Phys.* **1979**, *70*, 3300−3316.

(53) Clayden, N. J.; Dobson, C. M.; Lian, L.-Y.; Smith, D. J. *J. Magn. Reson. A* **1986**, *69*, 476−487.

(54) Harris, R. K.; Lawrence, S. E.; Oh, S.-W.; Das, V. G. K. *J. Mol. Struct.* **1995**, *347*, 309−320.

(55) The definitions, $\Delta\Delta = \sigma_{11} - [(\sigma_{22} + \sigma_{33})/2]$ and $\Delta\sigma = \sigma_{33} - [(\sigma_{11} + \sigma_{22})/2]$, have been adopted in this work. The convention used herein for the asymmetry parameter is $\eta = (\sigma_{22} - \sigma_{33})/(\sigma_{11} - \sigma_{iso})$ or $(\sigma_{22} - \sigma_{11})/(\sigma_{33} - \sigma_{iso})$ so that $0 \le \eta \le 1$. Span ($\Omega$) and skew ($\kappa$) have been suggested as an alternative convention, where $\Omega = \sigma_{33} - \sigma_{11} = \delta_{11} - \delta_{33} > 0$ and $\kappa = 3(\sigma_{iso} - \sigma_{22})/(\sigma_{33} - \sigma_{11}) = 3(\delta_{22} - \delta_{iso})/(\delta_{11} - \delta_{33})$. Skew, as opposed to the asymmetry parameter, has values between −1 and 1 and gives a clearer indication of the sense of the tensor asymmetry, *i.e.*, $\kappa = 1$ (axial, $\sigma_{11} = \sigma_{22} > \sigma_{33}$), $\kappa = 1$ (axial, $\sigma_{11} > \sigma_{22} = \sigma_{33}$), and $\kappa = 0$ (complete asymmetry, $\sigma_{11} \neq \sigma_{22} \neq \sigma_{33}$).

(56) Mason, J. *Solid State Nucl. Magn. Reson.* **1993**, *2*, 285−288.

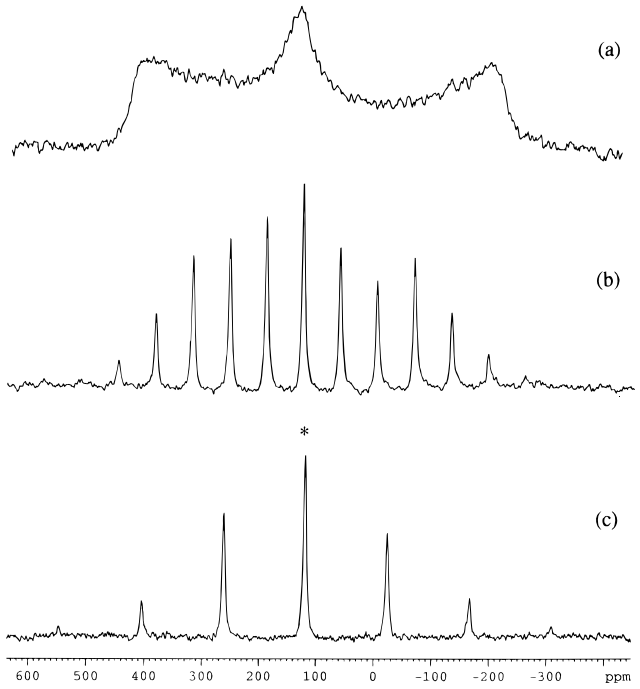


**Figure 4.** $^{171}$Yb spectra of **1** (a) Static, 9535 transients, S:N = 16; (b) RAMP-CP 4.5 kHz, 819 transients, S:N = 48; (c) RAMP-CP 10 kHz, 292 transients, S:N = 46.

**Table 2. Comparison of the Chemical Shift Tensor Data for 1 Derived From Spectra at the Following Conditions: (a) Static, (b) at 4.5 kHz, (c) at 10 kHz**

| | $\delta_{11}$ | $\delta_{22}$ | $\delta_{33}$ |
|---|---|---|---|
| **a** | 430 | 140 | −215 |
| **b**[a] | 432 | 145 | −208 |
| **b**[b] | 435 | 144 | −210 |
| **c**[a] | 424 | 127 | −196 |
| **c**[b] | 439 | 149 | −219 |

[a] See ref 52. [b] See ref 51.

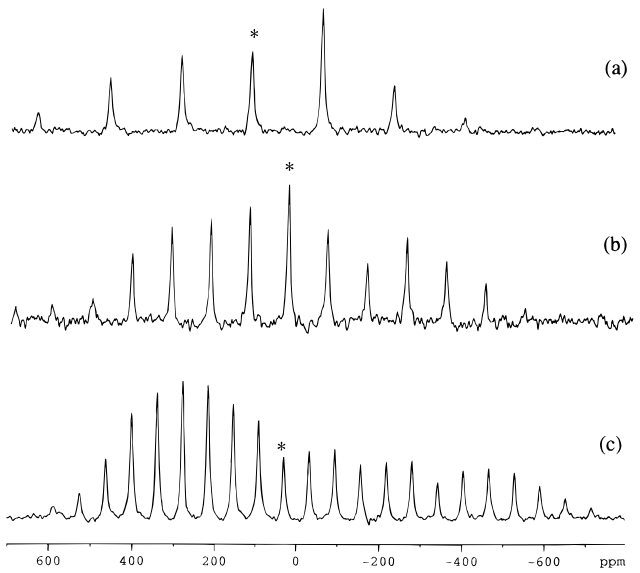


**Figure 5.** $^{171}$Yb spectra of (a) **4**, 12 kHz, 9024 transients; (b) **5**, 9.5 kHz, 908 transients; (c) **8**, 4.4 kHz, 5120 transients.

**Isotropic Chemical Shift and Chemical Shift Tensor Elements.** The isotropic chemical shifts of **1**−**9** are typical of $\pi$-bonded metal cyclopentadienyl derivatives in that they are of low-frequency compared with those containing $\sigma$-bonded ligands.[57] The line width at peak half-height, $\nu_{1/2}$, values are modest, 300−500 Hz, and are independent of rotation rate. The large $\nu_{1/2}$ for **3** is due to unresolved coupling to the two pyridine nitrogen atoms. Overall, again with the exception of **3**,[58] there is good agreement (±30 ppm) between the solid- and solution-state isotropic chemical shifts (Table 4). From an inspection of this data it is proposed that the isotropic chemical shift reflects: (i) The nature of the cyclopentadienyl ring substituents. The increased donor properties of $\eta$-$C_5Me_5$ compared to $\eta$-$C_5Me_4H$ result in a 130 ppm shift to lower frequency for **2** compared with **1**. (ii) The nature of the coordinating bases. The addition of a $\sigma$-bonded O- or N-centered Lewis base results in a deshielding of 30−50 ppm for the former, *e.g.*, **2**, and 300−400 ppm for the latter, *e.g.*, **3**. For a review of $^{171}$Yb solution-state chemical shift data, see ref 59. (iii) The Cp(centroid)−Yb−Cp(centroid) angle. Unlike all the other Yb derivatives examined, which exhibit a single isotropic chemical shift, **9** exhibits two at $\delta$ +34 and −36 ppm (Figure 6). A single-crystal X-ray diffraction analysis of **9** showed two independent molecules in the asymmetric unit with centroid−Yb−centroid angles of 145.0° and 145.7°.[29] The molecular structure of decamethylsilocene similarly exhibits two geometrical isomers, with (centroid)−Si−(centroid) angles of 180.0° and 167.4°. Their ratio, however, is 1:2, respectively, and therefore the two isotropic signals observed in the $^{29}$Si CP MAS, $\delta_{iso}$ −423 and −403, are easily assigned to the isomers possessing parallel and bent $C_5Me_5$ rings, respectively.[60,61] Additionally, the parallel isomer is also characterized by a slightly larger span and a lower asymmetry parameter. By analogy, the lower frequency resonance of **9** also exhibits both higher span and lower asymmetry and is therefore assigned to the geometrical isomer of **9** with the higher (centroid)−metal−(centroid) angle.

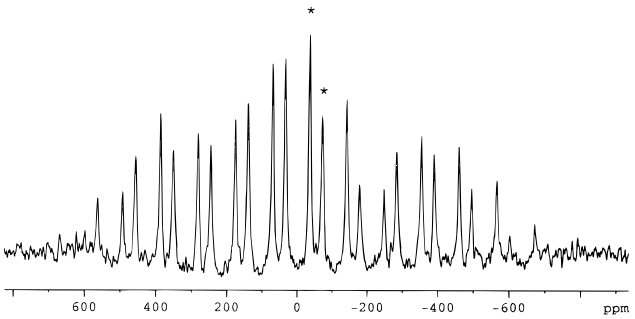


**Figure 6.** The $^{171}$Yb spectrum of **9** at $\nu_r$ = 7.5 kHz, 1202 transients, asterisk (*) denotes isotropic shift.

Despite the chemical shift dispersion associated with $^{171}$Yb NMR spectroscopy, accidental coincidence of the isotropic chemical shifts may occur, *e.g.*, as for **5** and **7**; when the $\pi$-ligands are changed from $\eta$-$C_5Me_4SiMe_3$ to $\eta$-$C_5Me_5$, the isotropic chemical shift remains unchanged. From an inspection of the tensor elements, however, it is evident that this results from equal but opposite changes in $\delta_{11}$ and $\delta_{22}$ (by *ca.* 100 ppm,

(57) Wrackmeyer, B. *Annu. Rep. NMR Spectrosc.* **1985**, *16*, 73−186.
(58) The high-frequency shift for **3** is postulated to result from a solution equilibrium between the bis and tris pyridine adducts.[24]
(59) Keates, J. M.; Lawless, G. A. $^{171}$Yb NMR Spectroscopy. In *Advanced Applications of NMR to Organometalic Chemistry*; Gielen, M., Willem, R., Wrackmayer, B., Eds.; J. Wiley & Sons: Chichester, 1996; Chapter 12, pp 357−370.
(60) Jutzi, P.; Kanne, D.; Kruger, C. *Angew. Chem., Int. Ed. Engl.* **1986**, *25*, 164.
(61) Wrackmeyer, B.; Sebald, A.; Merwin, L. H. *Magn. Reson. Chem.* **1991**, *29*, 260−263.

**Table 3. Chemical Shift Tensor Data and Values for Anisotropy, Asymmetry Parameter, Span, and Skew**

| | $\delta_{11}$ | $\delta_{22}$ | $\delta_{33}$ | $\Delta_\Delta$ | $\Delta_\sigma$ | $\eta$ | $\Omega$ | $\kappa$ |
|---|---|---|---|---|---|---|---|---|
| **1**[a] | 432 | 145 | −208 | 464 | 497 | 0.87 | 640 | 0.10 |
| **2**[a] | 334 | 79 | −341 | 465 | 548 | 0.70 | 675 | 0.24 |
| **3**[a] | 1298 | 669 | 379 | 774 | 605 | 0.56 | 919 | −0.37 |
| **4**[a] | 689 | 32 | −337 | 842 | 698 | 0.66 | 1026 | −0.28 |
| **5**[a] | 535 | 71 | −520 | 760 | 823 | 0.85 | 1055 | 0.12 |
| **6**[a] | 592 | −34 | −488 | 854 | 767 | 0.80 | 1080 | −0.16 |
| **7**[b] | 648 | −55 | −508 | 930 | 805 | 0.73 | 1156 | −0.22 |
| **8**[a] | 533 | 261 | −704 | 755 | 1101 | 0.37 | 1237 | 0.56 |
| **9**[a] | 644 | 50 | −595 | 916 | 942 | 0.95 | 1239 | 0.04 |
| | 562 | 14 | −686 | 898 | 974 | 0.85 | 1248 | 0.12 |

[a] This work. [b] Reference 25.

**Table 4. Solution Chemical Shifts, Solid-State Isotropic Chemical Shifts, and Line Widths at Half-Height for 1−9**

| compound | solution chemical shift (ppm) | $\delta_{iso}$ (ppm) | $\nu_{1/2}$ (Hz) |
|---|---|---|---|
| Yb($\eta$-$C_5Me_4H)_2(THF)_2$, **1**[a] | 131 (THF) | 123 | 300 |
| [Yb($\eta$-$C_5Me_5)_2(THF)_2$], **2** | 0 (THF)[c] | 24 | 170 |
| [Yb($\eta$-$C_5Me_5)_2(py)_2$], **3** | 949 (py)[c] | 783 | 1000 |
| [Yb($\eta$-$C_5Me_5)_2$(DME)], **4**[a] | 98 (DME/bz)[d] | 128 | 500 |
| [Yb{$\eta$-$C_5Me_4(SiMe_3)\}_2$THF], **5**[a] | 6 (THF) | 28 | 250 |
| [Yb($\eta$-$C_5Me_5)_2(OEt_2)$], **6** | 26 ($Et_2O$)[c] | 23 | 300 |
| [Yb($\eta$-$C_5Me_5)_2$(THF)·$^1/_2$PhMe], **7**[e] | | 28 | *f* |
| [Yb{$C_5Me_4(SiMe_2Bu^t)\}_2$], **8**[a] | 20 ($C_7H_{14}$) | 30 | 250 |
| [Yb($\eta$-$C_5Me_5)_2]_\infty$, **9**[b] | −33 (PhMe)[g] | 34[h] | 170 |
| | | −36 | 300 |

[a] This work. [b] Reference 24. [c] Reference 13. [d] Reference 28. [e] Reference 25. [f] Not stated in ref 25. [g] Reference 32. [h] Two independent molecules in the asymmetric unit.

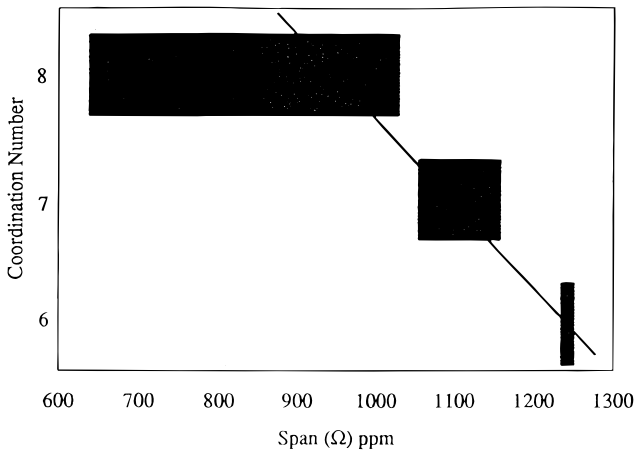


**Figure 7.** Correlation between Ω and coordination number.

respectively), whereas $\delta_{33}$ remains virtually unchanged. Thus, we propose that $\delta_{11}$ and $\delta_{22}$ are orientated toward the cyclopentadienyl rings while $\delta_{33}$ is directed toward the coordinating bases. Consequently, the decrease in $\delta_{33}$ on going from **1** to **9** mirrors a decrease in the formal coordination number, CN, at the Yb center. This trend is reflected more clearly when $\Delta_\sigma$ or Ω are calculated for **1**−**9**; thus, for CN = 8, Ω = 800−900, for CN = 7, Ω = 1050−1150, and for CN = 6, Ω = 1150−1250 (Figure 7). Two anomalies in this series merit discussion. First, the high Ω value exhibited by **4**, which indicates a CN lower than 8, and second the very low Ω values for **1** and **2**, indicating a CN higher than 8. For **4**, the high Ω value reflects the smaller O−Yb−O angle associated with the bidentate DME ligand (*ca.* 66−67°) compared to the corresponding angle associated with bis(monodentate) O- and N-centered Lewis bases (*ca.* 82−84°). Second, although for **1** and **2**[62] the isotropic chemical shifts differ by some 100 ppm, the similarity between the skew values implies an identical coordination number. The low Ω values exhibited by **1** and **2** compared to the other eight-coordinate compounds **3** and **4** can be explained by considering each of the two THF bases not as two-electron donors but as four-electron $\pi$-donors,[63] thereby effectively increasing the coordination number and thus decreasing Ω. Therefore, although the molecular structures of **1** and **2** have not been reported, they are predicted to resemble [Sm($\eta$-$C_5Me_5)_2(THF)_2$], in which the two THF ligands do not adopt the planar conformation typically observed for compounds possessing one THF ligand but rather a half-chair conformation. Finally, the values for the asymmetry parameter and $\kappa$ follow no obvious trend. With the exception of **8**, all values are larger than 0.5 and typical of low-symmetry systems.

## Conclusion

[Yb($\eta$-$C_5Me_5)_2(THF)_2$] is proposed as the standard for $^{171}$Yb CP MAS NMR spectroscopy. The proton $T_{1\rho}$ values have been determined and are comparable to those found in other organometallic systems. Either single contact CP or, at elevated spin rates, RAMP-CP provide high S:N spectra within moderate acquisition times. While $\delta_{iso}$ is best regarded as an indication of the overall electronic effect of the ligand set, the values of $\delta_{33}$ reflect the nature and geometry of the coordinating bases and those of $\delta_{11}$ and $\delta_{22}$ the nature of the cyclopentadienyl ring substituents. Thus, the coordination and subsequent activation of small molecules should predominately result in changes in $\delta_{33}$. Although the chemical shift anisotropy in these systems is moderately large, it is not sufficiently so as to prevent the implementation of $^{171}$Yb CP MAS NMR spectroscopy, particularly at fields lower than 9.4 T, as a routine tool in the exploration of the structure and reactivity associated with ytterbium(II) organometallic derivatives.

OM9700223

(62) An alternative set of chemical shift tensor data for **2** has been reported ($\delta_{11}$ = 321, $\delta_{22}$ = 60, $\delta_{33}$ = −293).[25] The lower S:N ratio of this data precludes an accurate comparison of this data.

(63) Jordan, R. F.; Bajgur, C. S.; Willett, R.; Scott, B. *J. Am. Chem. Soc.* **1986**, *108*, 7410−7411.